PHYSICAL REVIEW B VOLUME 4, NUMBER 12 15 DECEMBER 1971

Lattice Dynamics of CsBr

Stig Rolandson*
Physics Department, Chalmers University of Technology, Gothenburg, Sweden
and
Gerhard Raunio
Physics Department, University of Linköping, Linköping, Sweden
(Received 24 June 1971)

The phonon dispersion curves of cesium bromide have been observed by inelastic neutron scattering in the symmetry directions Δ, Σ, and Λ and along the symmetry line T. The measurements were performed at 80 and 300 K using a three-axis crystal spectrometer. The observations have been fitted to various versions of the shell model, and the frequency distribution and the temperature dependence of the Debye temperature have been calculated from the model which gives the best fit to the experimental frequencies.

I. INTRODUCTION

The lattice dynamics of alkali halides have been subject to a great deal of theoretical and experimental effort during recent years. Various dynamical models of the microscopic interactions have been developed[1-5] and the agreement with experimental results has been quite good. The most powerful method of studying lattice dynamics is inelastic scattering of thermal neutrons. This technique has been used to obtain phonon dispersion curves for most of the alkali halides with NaCl structure,[6-16] and theoretical models such as the shell model and the breathing-shell model have been rather successful in describing the experimental data. One of the aims of the present work was to investigate the applicability of these models to CsBr which has the CsCl structure. No inelastic neutron data existed for an alkali halide with this structure when these measurements started. However, simultaneously and independently CsBr was studied by the time-of-flight technique by Daubert.[17] The reported results for the [100] direction at room temperature agree well with our measurements.

An interesting property of CsBr is that the anharmonic contribution to the heat capacity is large and negative compared with the alkali halides with NaCl structure.[18] This difference cannot be explained by simple theories and detailed knowledge of the dispersion relations and the frequency distribution is certainly valuable in the future study of this problem.

In Sec. II we briefly describe the experimental technique and give the measured frequencies in the symmetry directions. A short discussion of the models is given in Sec. III together with the results of the least-squares fitting to the phonon frequencies.

The 11-parameter shell model of Woods *et al.*[1] is used in Sec. IV to generate the frequency distribution and the temperature dependence of the Debye temperature in the harmonic approximation.

II. EXPERIMENTAL AND RESULTS

The sample was a single crystal of dimensions $2.5\times2.5\times5$ cm and a mosaic width of about 1° full width at half-maximum (FWHM). Such a relatively large mosaic width and the high absorption of the crystal (20–30 b) make measurements especially difficult, and special care had to be taken when choosing the experimental conditions for a specific run. The phonons observed were well resolved and in the analysis of the experimental data we used as a rule two measurements of the same phonon resonance from different points in reciprocal space. The experiment was performed at the R2 reactor at Studsvik using one of the double-monochromator spectrometers described by Stedman *et al.*[19] To monochromatize the beam we used exclusively the (220) planes of two copper crystals and the scattered neutrons were analyzed either by Cu (220) or Cu (111). The horizontal collimations before and after the sample were 0.0095 and 0.02 rad, respectively, and the vertical collimation was twice as large. Throughout the experiment the spectrometer was run in the "constant-κ" mode of operation and phonon creation was observed. Optimum conditions for focusing[20] could only be obtained in a few cases because of the small slope of the dispersion curves, and the focusing technique was in most cases used only as a guide to choose the most favorable beam path and κ vector. Inelastic structure factors, calculated from the eigenvectors of the DD^+ model of Karo,[21] were used to select appropriate regions in reciprocal space where good intensity could be expected. Most of the measurements were done at liquid-nitrogen temperature while less extensive measurements were done at room temperature. The major part of the phonons were observed with the crystal oriented with

a $[1\bar{1}0]$ direction perpendicular to the scattering plane, but for the transverse phonons in the Σ directions with polarization in the $[1\bar{1}0]$ direction we used a scattering plane perpendicular to [001].

The dispersion curves have been determined in the high-symmetry directions Δ, Σ, and Λ, and along the symmetry line T (see Table I). Some selected phonons have also been measured at room temperature and a special effort has been devoted to obtain the phonons at the points Γ, R, M, and X, as these phonons play an important role in second-order Raman scattering (see Table II). The phonon resonances were analyzed by using the method of Stedman and Weymouth[22] and the experimental errors so obtained are generally between 1 and 2%, but for some of the lowest energy acoustic phonons the errors are 4–5%. In these cases the relatively large mosaic width of the crystal caused a slooping background of elastically scattered neutrons which had to be subtracted before analyzing the phonon resonance, and this gave an extra contribution to the error of the phonon frequency. The relative uncertainties are generally somewhat larger for CsBr than in earlier measurements on alkali halides[10–16] using the same spectrometer. This is due to the combined effect of the high absorption and the rather broad mosaic width of the specimen.

III. MODELS

The shell model of Woods *et al.*[1] and the breathing-shell model (BSM) of Schröder[3] have been used to relate the neutron results to microscopic inter- and intra-ionic interactions in the crystal. The most generalized versions of these models contain 29 parameters when second-nearest-neighbor interactions are included.[23] By doing some approximations, which seem reasonable from a physical point of view, this fairly large number of parameters is reduced to between seven and eleven for the four different models used here to describe the lattice dynamics of CsBr. The adjustable parameters are determined from the measured phonon frequencies in the high-symmetry directions by a least-squares fitting procedure. The quality of the fit is given by the quantity χ^2 defined as

TABLE I. Phonon frequencies in CsBr at 80 K.

Direction	Wave vector $aq/2\pi$	Phonon frequencies (10^{13} rad sec^{-1})					
		TA	LA	TO	LO		
[100]	0	•••	•••	1.440 ±0.015	•••		
(Δ)	0.1	•••	0.397 ±0.006	1.45 ±0.03	2.10 ±0.03		
	0.2	0.37 ±0.02	0.785 ±0.010	1.35 ±0.02	2.05 ±0.03		
	0.3	0.555 ±0.010	1.080 ±0.015	1.28 ±0.01	1.99 ±0.03		
	0.4	0.710 ±0.015	1.29 ±0.02	1.25 ±0.01	1.88 ±0.02		
	0.5	0.845 ±0.015	1.44 ±0.04	1.21 ±0.01	1.83 ±0.03		
		TA	LA	TO	LO		
[111]	$0.05\sqrt{3}$	•••	•••	•••	2.12 ±0.03		
(Λ)	$0.1\sqrt{3}$	0.360 ±0.015	0.628 ±0.010	1.440 ±0.015	2.01 ±0.02		
	$0.2\sqrt{3}$	0.685 ±0.010	1.08 ±0.02	1.470 ±0.015	1.705 ±0.015		
	$0.3\sqrt{3}$	0.910 ±0.015	1.16 ±0.02	1.49 ±0.02	1.58 ±0.02		
	$0.4\sqrt{3}$	1.075 ±0.020	1.10 ±0.02	1.520 ±0.015	1.58 ±0.02		
	$0.5\sqrt{3}$	1.17 ±0.03	1.17 ±0.03	1.53 ±0.02	1.53 ±0.02		
		T_2A	T_1A	LA	T_2O	T_1O	LO
[110]	$0.05\sqrt{2}$	•••	•••	•••	•••	•••	2.12 ±0.04
(Σ)	$0.1\sqrt{2}$	•••	0.280 ±0.015	•••	1.49 ±0.01	1.39 ±0.01	2.015 ±0.020
	$0.2\sqrt{2}$	0.61 ±0.01	0.537 ±0.007	0.970 ±0.015	1.54 ±0.02	1.30 ±0.02	1.88 ±0.01
	$0.3\sqrt{2}$	0.815 ±0.015	0.715 ±0.010	1.18 ±0.02	1.61 ±0.02	1.22 ±0.02	1.64 ±0.03
	$0.4\sqrt{2}$	0.970 ±0.015	0.775 ±0.015	1.04 ±0.02	1.67 ±0.02	1.130 ±0.015	1.66 ±0.03
	$0.5\sqrt{2}$	1.01 ±0.02	0.77 ±0.02	1.01 ±0.02	1.69 ±0.03	1.11 ±0.03	1.69 ±0.03
	ζ	TA	LA	TO	LO		
$[\frac{1}{2}\frac{1}{2}\zeta]$	0.125	0.85 ±0.02	•••	1.25 ±0.02	•••		
	0.250	0.99 ±0.02	•••	1.39 ±0.03	1.64 ±0.03		
(T)	0.375	1.10 ±0.02	•••	•••	•••		

TABLE II. Phonon frequencies in CsBr at 300 K.

Direction	Wave vector $aq/2\pi$	Phonon frequencies (10^{13} rad sec^{-1})					
		TA	LA	TO	LO		
[100]	0	•••	•••	1.40±0.02	•••		
(Δ)	0.3	0.528±0.007	1.13±0.02	1.21±0.02	1.93±0.03		
	0.5	0.785±0.015	•••	1.10±0.03	1.75±0.02		
[111]		TA	LA	TO	LO		
(Λ)	$0.5\sqrt{3}$	•••	1.13±0.02	•••	1.50±0.02		
		T_2A	T_1A	LA	T_2O	T_1O	LO
[110]	$0.2\sqrt{2}$	0.595±0.010	•••	1.02±0.02	1.46±0.02	•••	1.84±0.03
(Σ)	$0.5\sqrt{2}$	•••	0.74±0.02	0.97±0.02	•••	1.05±0.02	1.62±0.03

$$\chi^2 = \frac{1}{N-P} \sum_{i=1}^{N} \left(\frac{\nu_{ic} - \nu_i}{\sigma_i} \right)^2 ,$$

where N is the number of observations, P the number of adjustable parameters in the model, ν_i and ν_{ic} are the observed and calculated frequencies of the ith phonon, and σ_i its estimated experimental uncertainty. Another indication of the relevance of a specific model is the calculated values of the elastic and dielectric constants, which are not incorporated in the fitting.

Models I–III are similar to the shell model of Cowley *et al.*[24] Using the harmonic, adiabatic, and electrostatic approximations the equations of motion can be written

$$\omega^2 \underline{m}\ \underline{U} = (\underline{R} + \underline{Z}\,\underline{C}\,\underline{Z})\underline{U} + (\underline{T} + \underline{Z}\,\underline{C}\,\underline{Y})\underline{W} ,$$

$$O = (\underline{\tilde{T}} + \underline{Y}\,\underline{C}\,\underline{Z})\underline{U} + (\underline{\zeta} + \underline{Y}\,\underline{C}\,\underline{Y})\underline{W} ,$$

where $\underline{m}$, $\underline{Z}$, and $\underline{Y}$ are diagonal matrices representing the ion masses, the ion charges, and the shell charges, respectively. The short-range interactions of type core-core, core-shell, and shell-shell are given by the matrices $\underline{R}$, $\underline{T}$, and $\underline{\zeta}$, respectively, while $\underline{C}$ specifies the long-range Coulomb interactions. $\underline{U}$ and $\underline{W}$ are polarization vectors, $\underline{U}$ specifying the ionic displacements, and $\underline{Y}$ $\underline{W}$ the dipole moments of the ions. To reduce the number of adjustable parameters we followed Cowley *et al.*[24] by setting $\underline{R} = \underline{S} = \underline{T}$ for all wave vectors. $\underline{S}$ is defined through $\underline{\zeta} = \underline{S} + \underline{K}$, where $\underline{K}$ is a diagonal matrix whose elements k_1 and k_2 are the core-shell coupling constants for the positive and negative ion, respectively. Physically this means that all short-range forces act entirely through the shells. The short-range interaction is defined by the radial and tangential force constants A and B which we consider as adjustable parameters. The subscripts 1 and 2 refer to the positive and negative ions, respectively (see Table III).

The short-range potential between nearest neighbors is assumed to be noncentral and B'' is the noncentral component of the tangential force constant. The central component B_{12} is eliminated through the stability condition for the lattice.[25] The remaining parameters are the ionic charge

TABLE III. Parameters for the four shell modes which give the best fit to the experimental results. v is the volume of the primitive cell.

Model parameters	Units	Model I	II	III	IV
A_{12}	$e^2/2v$	8.85 ±0.22	8.85 ±0.37	8.39 ±0.49	8.04 ±0.67
A_{11}	$e^2/2v$	•••	•••	0.97 ±0.39	0.49 ±0.29
B_{11}	$e^2/2v$	•••	•••	−0.22 ±0.08	−0.15 ±0.06
A_{22}	$e^2/2v$	•••	−0.13 ±0.34	0.20 ±0.32	0.56 ±0.32
B_{22}	$e^2/2v$	•••	0.32 ±0.07	0.12 ±0.10	0.15 ±0.10
B''	$e^2/2v$	−0.15 ±0.08	−0.11 ±0.07	−0.29 ±0.08	−0.16 ±0.11
Z	e	0.943±0.016	0.953±0.035	0.849±0.057	0.85 ±0.06
α_1	10^{-24} cm^3	3.09 ±0.57	2.37 ±0.56	0.51 ±0.38	1.19 ±0.66
α_2	10^{-24} cm^3	1.76 ±0.65	1.91 ±0.50	1.72 ±0.53	2.10 ±0.67
d_1	e	−0.099±0.028	−0.104±0.040	−0.080±0.034	0.002±0.04
d_2	e	0.087±0.022	0.086±0.018	0.044±0.040	0.073±0.05
χ^2	•••	5.85	3.40	2.94	3.31

TABLE IV. Comparison of some physical quantities derived from the models and experimental data. The elastic constants are given in units of 10^{11} dyn/cm^2.

	Model				
	I	II	III	IV	Expt
C_{11}	3.50	3.44	3.49	3.30	3.345[a] 3.355[b]
C_{12}	1.07	1.04	1.30	1.00	0.966[a] 1.002[b]
C_{44}	0.85	0.89	0.89	0.88	0.951[a] 0.963[b]
ϵ_0	4.28	4.08	2.92	3.57	6.45[c]
ϵ_∞	2.05	1.88	1.41	1.64	2.81[d]

[a]See Ref. 27.
[b]See Ref. 28.
[c]See Ref. 34.
[d]See Ref. 35

Ze, and α_1, d_1 and α_2, d_2—the electrical and mechanical polarizabilities of the positive and negative ion, respectively.

Both types of ions are considered to be polarizable in all models, as the electronic polarizabilities of the Cs and Br ions are of the same order of magnitude (3.14 and 4.13 Å^{-3}, according to Tessman *et al.*[26]). Models I–III differ in respect to the short-range interaction between next nearest neighbors (see Table III). Model I, where the short-range potential extends only to nearest neighbors, gives a rather poor fit to the experimental frequencies, especially for the longitudinal acoustic phonons in the Δ and Σ directions. The short-range interactions between next nearest neighbors of the Br ions are included in model II, which makes the χ^2 value significantly lower, and the fit is further improved for model III, where the full short-range interaction between next nearest neighbors is assumed. The elastic constants derived from these models are in fair agreement with ultraonic measurements of Vallin *et al.*[27] and Reinitz,[28] as can be seen from Table IV. This consistency between calculated elastic constants and experimental results is not improved when the range of the short-range potential is increased beyond nearest neighbors. This is an indication that the force constants originating from next-nearest-neighbor interaction have a comparatively small influence on the elastic properties.

For all these models d_1 is negative, indicating that the electron shell of the Cs ion has a positive charge, which is physically unreasonable. In PbTe[23] and AgCl[29] the results were markedly improved by using a shell model where the approximation $R = T$ is relaxed and a direct core-shell interaction is introduced by the two additional parameters $\beta_T(12)$ and $\beta_T(21)$ defined as $T_{12} = \beta_T(12)R_{12}$ and $T_{21} = \beta_T(21)R_{21}$.

Such a model with 13 parameters was also examined for CsBr, but is in no respect superior to model III. The parameters $\beta_T(12)$ and $\beta_T(21)$ are close to 1, which shows the validity of the assumption that all short-range forces act only between the shells.

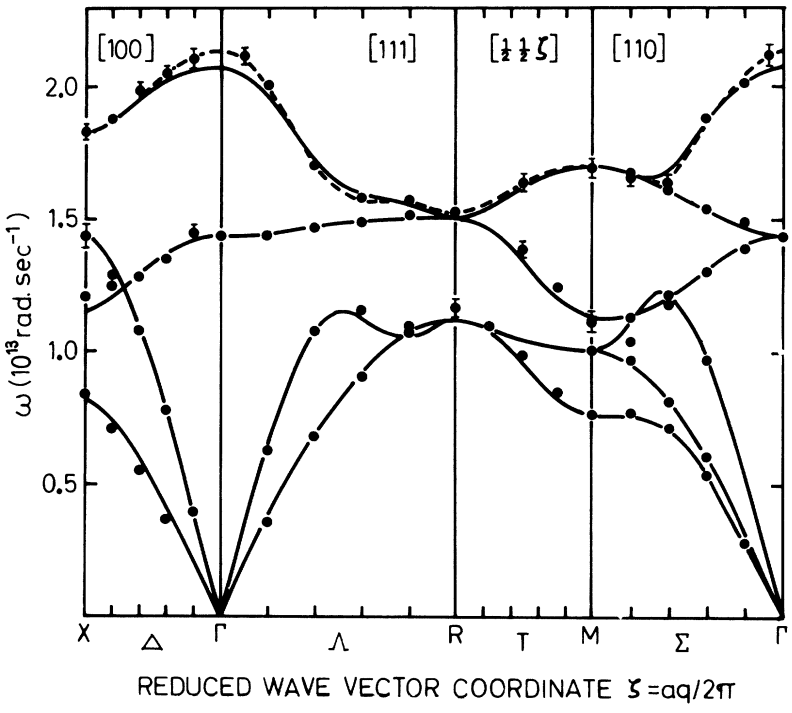

FIG. 1. Dispersion curves for CsBr at 80 K. The solid lines are the best least-squares fit to the results from model III and the broken lines show the LO branches according to model IV (BSM). Error bars are omitted for experimental points with uncertainties less than or comparable to the size of the dots.

Model IV is the BSM first proposed by Schröder[3] who modified the shell model by allowing the shells of the ions to be radially deformed or to "breath." This gives a new degree of freedom per ion represented by a breathing coordinate and associated with it a breathing force constant, which together determine the isotropic force acting on the shell due to a radial deformation. The total number of parameters is not increased by introducing the breathing interactions as the breathing force constants are set equal to the ones related to translational deformations of the ions, that is, k_1 for the positive and k_2 for the negative ion. A consequence of the BSM with central forces is that $c_{12} < c_{44}$.[30] This is not the case in CsBr and as in the rigid-shell model we have to introduce a noncentral force constant B'' to be able to obtain realistic elastic constants. Model IV has the same number of adjustable parameters as model III but the χ^2 value is somewhat larger. However, the fit to the LO phonons is significantly better, as is found in Fig. 1 where the dashed curves indicate the LO branches of model IV. For the other branches model III gives in most cases a better fit, but the difference between the two models is small. The elastic constants derived from model IV give the best agreement with ultrasonic results and d_1 has a physically acceptable value, which is not the case for the other models.

IV. DERIVED PROPERTIES

A. Frequency Distribution

Even if there is some minor discrepancies between model III and the measured phonon frequencies, this model is undoubtedly quite capable of generating an adequate frequency distribution for CsBr. The method of calculation is based on the approach of Gilat and Raubenheimer[31] suitably modified to the shell model. The irreducible part of the Brillouin zone was divided into small cubes and the phonon frequencies and their gradients were computed at the centers of each cube. A first-order Taylor expansion was then carried out around these points to generate constant-frequency planes through the cube which bound a volume with phonon states belonging to the same frequency channel. The contribution from each small cube to a specific channel of the frequency distribution is then proportional to the volume of the corresponding slice of the cube. The frequency distribution shown in Fig. 2 is based on 506 mesh points in the irreducible part of the Brillouin zone and the channel width is 0.01 $\times 10^{13}$ rad sec^{-1}. The uncertainties involved in the method were estimated by doing two independent calculations with the mesh of small cubes shifted with respect to each other. The maximum deviation was at the most a few percent, except for the low-frequency part. This originates from phonon states near the origin of the Brillouin zone where the curvature of the dispersion surfaces is appreciable, which makes our method of calculation less accurate.

B. Debye Temperature

The frequency distribution was used to calculate the Debye temperatures $\Theta_D(T)$ as a function of temperature. The result is shown in Fig. 3, together with results of Sorai[18] obtained from heat-capacity measurements. The two sets of data are in reasonable agreement if one considers that no corrections for anharmonic effects have been included in our calculation, which explains the deviation at higher temperatures.

At low temperatures $\Theta_D(T)$ is sensitive to the low-frequency part of the frequency distribution, where the relative errors are fairly large owing to the method of computation. The elastic constants calculated from model III were used to obtain $\Theta_D(0)$.[32] This is indicated in Fig. 3 with a filled circle.

V. DISCUSSION AND CONCLUSIONS

The least-squares fit to the measured frequencies for the different versions of the shell model is of the same quality as in similar calculations for alkali halides with NaCl structure.[13,16,33] The best agreement to neutron results was obtained for models III and IV, both containing 11 parameters, but model IV is slightly to be preferred as in this case no parameter has unphysical values and the calculated elastic constants are in better agreement with ultrasonic results. The calculated low- and high-frequency dielectric constants are given in Table IV. The values are consistently lower than the results from electromagnetic measurements, and the electrical polarizabilities α_1 and α_2 are also less than the values reported by Tessman *et*

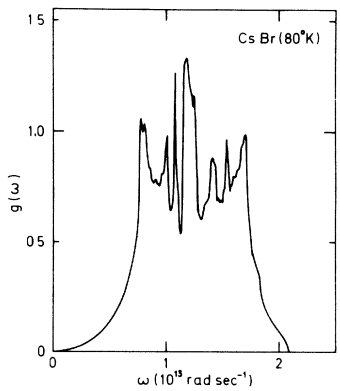

FIG. 2. Frequency distribution for phonons in CsBr calculated from model III.

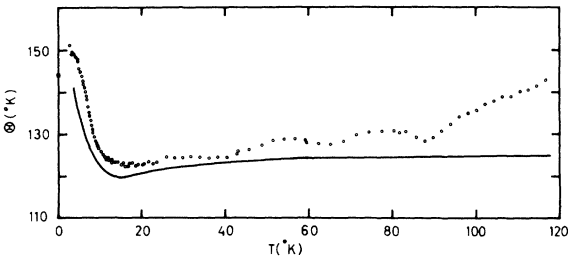

FIG. 3. Comparison of experimental (see Ref. 18) and calculated (model III) temperature dependence of the Debye temperature of cesium bromide.

al.[26] The observation that the best fit to the neutron data is obtained by using significantly lower polarizabilities for the ions than the values deduced from dielectric measurements indicates that the shell models overestimate the polarization effects on the phonon frequencies for CsBr. However, it must be stressed that this conclusion is based on a least-squares fitting procedure which gives rather large uncertainties for the parameters (Table III). Due to this fact it is not advisable to make a more physical interpretation of the variation of the parameters for the different models, even if some of these parameters seem to be rather model dependent.

The low- and high-frequency dielectric constants ϵ_0 and ϵ_∞ are related by the Lyddane-Sachs-Teller (LST) relation[34] to the frequencies of the transverse and longitudinal modes for $q=0$, ω_{TO}, and ω_{LO}, respectively, according to the formula $(\epsilon_0/\epsilon_\infty)^{1/2} = \omega_{LO}/\omega_{TO}$. This relation cannot be tested rigorously for CsBr in this experiment as there are no neutron data for ω_{LO} due to the well-known difficulties to measure this particular phonon.[10] A good estimation can, however, be obtained by using model IV (BSM) which gives the best fit to the LO branches. The result from this model for ω_{LO} at 80 K is 2.14×10^{13} rad sec^{-1}, which is in accordance with reflectance measurements on thin films by Lowndes,[35] who obtained 2.15×10^{13} rad sec^{-1}. The result from neutron measurements for ω_{TO} at 80 K is 1.440, which makes the ratio $\omega_{LO}/\omega_{TO} = 1.486$. Using 2.81 for ϵ_∞[36] and 6.45 for ϵ_0,[37] we obtain $(\epsilon_0/\epsilon_\infty)^{1/2} = 1.515$. The 2% difference is well within the estimated errors and the neutron data strongly support the validity of the LST relation in CsBr.

Lowndes[35] has determined ω_{TO} at 290 and 2 K by infrared transmission measurements. His values 1.39×10^{13} and 1.48×10^{13} rad sec^{-1} are in good agreement with the neutron results 1.40×10^{13} at 300 and 1.44×10^{13} rad sec^{-1} at 80 K.

ACKNOWLEDGMENTS

We are indebted to A. M. Karo for sending us results from numerical calculations on various theoretical models, and to R. P. Lowndes for communicating unpublished data. Professor H. P. Myers kindly supplied the sample crystal and also gave support in other respects. The authors are grateful to K. O. Isaxon for skillful technical assistance. One of us (G. R.) thanks the Swedish Atomic Research Council for a research grant.

*Present address: AB Atomenergi, Studsvik, Nyköping, Sweden.

[1]A. D. B. Woods, W. Cochran, and B. N. Brockhouse, Phys. Rev. 119, 980 (1960).
[2]A. M. Karo and J. R. Hardy, Phys. Rev. 141, 696 (1966).
[3]U. Schroder, Solid State Commun. 4, 347 (1966).
[4]M. P. Verma and R. K. Singh, Phys. Status Solidi 33, 769 (1969).
[5]S. Sinha, Phys. Rev. 177, 1256 (1969).
[6]A. D. B. Woods, B. N. Brockhouse, R. A. Cowley, and W. Cochran, Phys. Rev. 131, 1025 (1963).
[7]G. Dolling, R. A. Cowley, C. Schittenhelm, and I. M. Thorson, Phys. Rev. 147, 577 (1966).
[8]W. J. L. Buyers, Phys. Rev. 153, 923 (1967).
[9]G. Dolling, H. G. Smith, R. M. Nicklow, P. R. Vijayaraghavan, and M. K. Wilkinson, Phys. Rev. 168, 970 (1968).
[10]G. Raunio, L. Almqvist, and R. Stedman, Phys. Rev. 178, 1496 (1969).
[11]G. Raunio and L. Almqvist, Phys. Status Solidi 33, 1013 (1970).
[12]G. Raunio and S. Rolandson, J. Phys. C 3, 1013 (1970).
[13]G. Raunio and S. Rolandson, Phys. Status Solidi 40, 749 (1970).
[14]J. S. Reid, T. Smith, and W. J. L. Buyers, Phys. Rev. B 1, 1833 (1970).
[15]W. Bührer, Phys. Status Solidi 41, 789 (1970).
[16]S. Rolandson and G. Raunio, J. Phys. C 4, 958 (1971).
[17]J. Daubert, Phys. Letters 32A, 438 (1970).
[18]M. Sorai, J. Phys. Soc. Japan 25, 421 (1968).
[19]R. Stedman, L. Almqvist, G. Raunio, and G. Nilsson, Rev. Sci. Instr. 40, 249 (1969).
[20]R. Stedman, Rev. Sci. Instr. 39, 878 (1968).
[21]A. M. Karo (private communication).
[22]R. Stedman and J. Weymouth, Brit. J. Appl. Phys. 2, 903 (1969).
[23]W. Cochran, R. A. Cowley, G. Dolling, and M. M. Elcombe, Proc. Roy. Soc. (London) A293, 433 (1966).
[24]R. A. Cowley, W. Cochran, B. N. Brockhouse, and A. D. B. Woods, Phys. Rev. 131, 1030 (1963).
[25]E. W. Kellermann, Phil. Trans. Roy. Soc. London A238, 513 (1941).
[26]J. R. Tessman, A. H. Kahn, and W. Shockley, Phys. Rev. 92, 890 (1953).
[27]J. Vallin, O. Beckman, and K. Salama, J. Appl. Phys. 35, 1222 (1964).
[28]K. Reinitz, Phys. Rev. 123, 1615 (1961).
[29]P. R. Vijayaraghavan, R. M. Nicklow, H. G. Smith, and M. K. Wilkinson, Phys. Rev. B 1, 4819 (1970).
[30]M. J. L. Sangster, G. Peckham, and D. H. Saunderson, J. Phys. C 3, 1026 (1970).
[31]G. Gilat and L. J. Raubenheimer, Phys. Rev. 144,

390 (1966).
[32]L. De Launay, J. Chem. Phys. 30, 91 (1959).
[33]G. Raunio and S. Rolandson Phys. Rev. B 2, 2098 (1970).
[34]R. H. Lyddane, R. G. Sachs, and E. Teller, Phys. Rev. 59, 673 (1941).
[35]R. P. Lowndes, Phys. Rev. B 1, 2754 (1970).
[36]R. P. Lowndes and D. H. Martin, Proc. Roy. Soc. (London) A308, 473 (1969).
[37]R. P. Lowndes and D. H. Martin (private communication).

PHYSICAL REVIEW B VOLUME 4, NUMBER 12 15 DECEMBER 1971

Elastic Constants of the CsCl Structure Containing Impurity Ions

K. M. Kesharwani and Bal K. Agrawal
Physics Department, University of Allahabad, Allahabad-2, India
(Received 13 May 1971)

The T-matrix method has been used in determining the effect of point defects on the elastic properties of the crystals having a CsCl structure. The expressions for the bulk elastic constants have been obtained in terms of the local changes in the central- and the noncentral-force constants. A numerical estimate has been made in the case of CsI containing some impurity ions such as Rb^+, K^+, Tl^+, and In^+. The necessary force-constant changes have been taken from the results of the infrared lattice-absorption experiments. The calculated elastic constants have been tentatively compared with the experimentally measured elastic constants of a dilute alloy Mo-Re which has a bcc structure. Agreement is seen in the relative magnitudes of change in the elastic constants.

I. INTRODUCTION

The elastic properties of a crystal containing a finite concentration of defects are significantly altered. The local strains around the defect are seen to be different from that of the host lattice. A knowledge of these strains, induced locally by the applied stress, is required to interpret a number of experimental measurements of the effects of elastic strains[1-4] and electric fields[5] on the properties of crystals containing point defects. The bulk elastic constants are also modified.[6,7] The T-matrix method includes in a natural way the peculiarities of the discrete structure of the lattice. The method was discussed with a statistical approach by Elliott *et al.*,[8] who showed that the results obtained were similar to those of the dynamical approach.[9] Benedek and Nardelli[10] have applied the T-matrix method to discuss the influence of defects in alkali halides; however, they did not make any numerical estimate for the modified bulk elastic constants.

In the present paper, we use the T-matrix method for determining the effect of substantial point defects on the elastic properties of the crystals of CsCl structure. Expressions for the bulk elastic constants have been obtained in terms of local change of central- and noncentral-force constants. Numerical estimates have been made in the case of CsI containing some impurity ions such as Rb^+, K^+, Tl^+, and In^+. They are compared with the available experimental measurements of elastic constants of a bcc dilute Mo-Re alloy. The changes in the central- and noncentral-force constants deduced from the infrared lattice-absorption data[11,12] have been used.

II. THEORY

Let us consider a solid containing a low fractional concentration p of similar substitutional point defects. In order to understand the lattice dynamics of the imperfect solid, one must evaluate the perturbed phonon propagator or Green's function which is defined by

$$\underline{G}(z) = [\underline{L}_0 + \underline{P}_{s.c.}(\omega^2) - z\underline{I}]^{-1}, \tag{1}$$

where $\underline{L}_0$ is the mass-reduced dynamical matrix of the perfect host lattice and $\underline{P}_{s.c.}(\omega^2)$ is the perturbation matrix caused by a specific configuration of defects. For the explicit forms of these matrices, we refer to an earlier paper.[13] $z = \omega^2 + 2i\omega\zeta^+$ is the complex squared frequency in the limit as $\zeta^+ \to 0^+$. The propagator defined by Eq. (1) has been written for a single specific configuration of defects. If a statistical average over all the possible configurations of defects is taken, the averaged perturbed Green's function is given by

$$\langle \underline{G}(z) \rangle = \underline{G}^0(z) - \underline{G}^0(z)\,\underline{\Sigma}\,\langle \underline{G}(z) \rangle, \tag{2}$$

where the self-energy $\underline{\Sigma}$ is periodic like the perfect phonon propagator $\underline{G}_0$. Because of the configuration average, we can, therefore, go to the normal-mode representation and write

$$\langle G(\vec{k}) \rangle = [\omega^2_{\vec{k},s} + \Sigma(\vec{k}, s) - z]^{-1}, \tag{3}$$

where $\omega^2_{\vec{k},s}$ denotes the squared frequency of the